

# Localization and interference induced quantum effects at low magnetic fields in InGaAs/GaAs structures

A. P. Saveliev, Yu. G. Arapov, S. V. Gudina, V. N. Neverov, S. M. Podgornykh,  
N. G. Shelushinina, and M. V. Yakunin

*M. N. Miheev Institute of Metal Physics of the Ural Branch of the Russian Academy of Sciences  
Ekaterinburg 620108, Russia  
E-mail: saveliev@imp.uran.ru*

Received September 29, 2020, published online November 24, 2020

The longitudinal  $\rho_{xx}(B, T)$  and Hall  $\rho_{xy}(B, T)$  resistances are experimentally investigated in  $n$ -InGaAs/GaAs nanostructures with a single and double quantum wells in the magnetic field range  $B = 0$ –2.5 T and temperatures  $T = 1.8$ –20 K. It is shown that the origin of the temperature-independent point located at  $\omega_c \tau \cong 1$  on the  $\rho_{xx}(B, T)$  curves is due to the combined action of the classical cyclotron motion and the quantum interference effects of weak localization and electron-electron interaction. The results obtained indicate that the transition from the dielectric phase to the phase of the quantum Hall effect is a crossover from weak localization (quantum interference effects in a weak magnetic field) to strong localization in quantizing magnetic fields in the quantum Hall effect regime.

Keywords: quantum Hall effect, crossover, quantum interference.

## Introduction

The discussion about the fate of delocalized states responsible for transitions between different plateaus of the quantum Hall effect with decreasing magnetic field  $\mu B = \omega_c \tau \ll 1$  has a long history [1–5] and remains in the spotlight for lack of microscopic theory of the quantum Hall effect (QHE) [4] ( $\omega_c = eB / m^*$ ,  $n_c$ ,  $m^*$ ,  $\tau = l / V_F$ ,  $l$  and  $\mu$  being concentration, effective mass, transport time, mean free path and mobility of carriers, respectively). The main question is whether the disappearance (floating up) of delocalized states occurs during the quantum phase transition or it is explained by the crossover from weak localization (quantum interference effects in a weak magnetic field) to strong localization in the QHE regime [3, 5]. From a historical point of view, the theoretical concepts were based on the global QHE phase diagram [3], where the existence of delocalized states in strong magnetic fields can be consistent with the absence of delocalized states in zero magnetic field predicted by the scaling theory of localization in the 2D case [6], only if delocalized states float up above the Fermi energy when the magnetic field decreases to zero (the “floating up” hypothesis) [1, 2]. The new theoretical and experimental works shown both the floating up of delocalized states (see, references in [4, 5]) and the antilevitation [7 and references therein] when the energies of delocalized states turn out to be lower than the energies

of Landau levels related to ideal system with an increase in the degree of disorder  $W$ , or an increase in the magnetic field strength  $B$ .

It was shown [5] that QHE behavior (with  $\nu > 2$ ) in systems of finite dimensions at finite temperatures in the region of weak magnetic fields is well described by the scaling theory of QHE without using any exotic hypotheses like the floating up hypothesis. In [5] it was pointed out that there are some physical limits in observation of delocalized state floating up like the large localization length  $\xi$  which in a magnetic field in 2D systems puts the bounds in the form of exponentially low temperatures and exponentially large sizes of the system. The Hall resistance will be a monotonously increasing function of the magnetic field at achievable temperatures and system sizes. The temperature dependence of the dissipative resistance near the magnetic field values  $\omega_c \tau = 1$  changes from a weak increase in low magnetic fields to a decrease in high magnetic fields. Thus, the transition from dielectric behavior in zero magnetic field to the appearance of delocalized states in the QHE regime occurs through a crossover between weak localization at  $\omega_c \tau < 1$  and strong localization in a quantizing magnetic field.

Usually the so-called temperature-independent point ( $T_{\text{ind}}$ -point) on the magnetoresistance curves measured at different fixed temperatures serves as a boundary which divides the regions of magnetic fields where delocalized

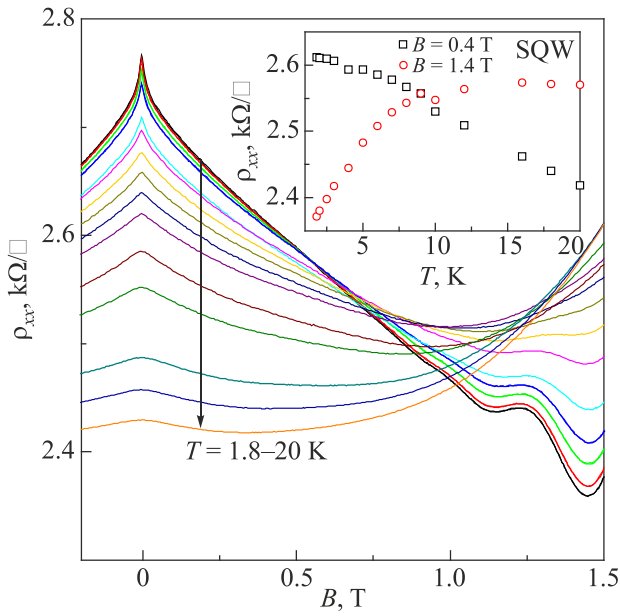


Fig. 1. (Color online) Dependencies  $\rho_{xx}(B)$  at  $T = (1.8-20)$  K for SQW. Inset shows the temperature dependences of  $\rho_{xx}$  at fixed magnetic fields  $B = 0.4$  T ( $\square$ ) and  $B = 1.4$  T ( $\circ$ ).

states are absent and where delocalized states are responsible for the appearance of transitions between quantized QHE plateaus. The well-defined  $T_{\text{ind}}$ -point was observed in the series of experiment in GaAs [8–12], quantum wells in the base of InAs [13–15], graphene [16, 17], Ge [18, 19] 2D systems. Mainly the position of  $T_{\text{ind}}$ -point doesn't coincide with the magnetic field value which is the boundary between classical and quantizing magnetic fields. Moreover, the  $T_{\text{ind}}$ -point position depends on carrier density [8, 13].

There are the works, which focused their attention on studying interaction-induced effects [8, 14] and the role of disorder potential scale on the  $T_{\text{ind}}$ -point position, and so insulator-quantum Hall liquid transition [8]. It can be easily noted that there is no clarity in this question and the most of the work has been done on the most perfect GaAs based system. In particular, for the GaAs/AlGaAs samples with long-range disorder potential, which is used as a tool for suppression of electron-electron interactions it was shown that  $B_c$  value didn't coincide with the onset of strong localization in QHE regime [8]. On the other hand, in the GaAs/AlGaAs quantum wells with the built-in layer of self-assembled InAs quantum dots, which is highly disordered it was made the conclusion that the critical point of metal-insulator transition didn't correspond to crossover points from localization to Landau quantization [13]. Therefore, it is quite interesting problem to study the system with a short-range disorder potential and a strong interference effects.

The scaling properties of the magnetoresistance at the  $T_{\text{ind}}$ -point were studied in [9–18] in the context of a quantum phase transition from the dielectric state to the QHE phase occurs. There is a point of view that the nature of the  $T_{\text{ind}}$ -point is associated with the joint action of classical

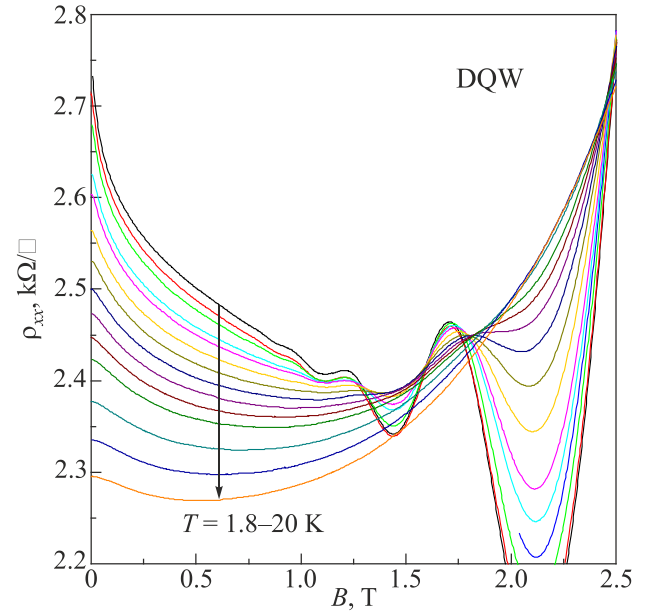


Fig. 2. (Color online) Dependencies  $\rho_{xx}(B)$  at  $T = (1.8-20)$  K for DQW.

cyclotron motion and quantum interference effects [19]. The interpretation of the experimental data (Figs. 1 and 2) within the scaling concept was presented in [15].

The aim of this work is to analyze the origin of the temperature-independent point on the  $\rho_{xx}(B, T)$  curves in low magnetic fields in the model of parabolic negative magnetoresistance in  $n$ -InGaAs/GaAs nanostructures in order to obtain a new information on the nature of transition from the dielectric phase to the phase of the quantum Hall effect.

### Experimental results and discussion

The  $n$ -In<sub>0.2</sub>Ga<sub>0.8</sub>As/GaAs samples were grown by organometallic gas-phase epitaxy on semi-insulating GaAs substrates at the Research Institute of Physics and Technology of Nizhny Novgorod University by the group of B. N. Zvonkov. The results obtained on the same samples as in [15] is discussed. The structures were symmetrically doped in Si barriers ( $n_D = 10^{18}$  cm<sup>-2</sup>), spacer width  $d_s = 19$  nm. The two types of structures are taken for the experiments with the same technological parameters: single (SQW) and double (DQW) quantum wells (see Table 1). The potential profiles of the studied systems, as a function of the growth direction  $z$ , were obtained from self-consistent solutions of Schrödinger and Poisson equations [20]. In a double tunnel-coupled quantum well the wave functions of the energy levels of each of the two wells are strongly mixed and form symmetric (S) and antisymmetric (AS) states separated by the tunnel gap  $\Delta_{SAS}$ . It follows from the calculations that two subbands, both of S and AS states, are filled in DQW samples. There is also only one filled subband in the SQW sample. One can see a quite close parameters of charge carriers and structures (Table 1). The ratio of transport

mean free time  $\tau_{tr}$  to quantum life time  $\tau_q$ , which characterize the scale of disorder potential is  $\tau_{tr}/\tau_q \approx 1$ . This is an indicator of a short-range disorder potential and agree well with the fact that we deal with the predominantly short-range scattering potential from the alloy scattering of electrons by In atoms as substitutional impurities. Rather high values of the parameter,  $k_F l \gg 1$ , indicate the good quality of the samples studied. Effective mass of charge carriers  $m^* = 0.058m_0$ , where  $m_0$  is the mass of a free electron.

Table 1. Parameters of the samples:  $d_w$  is the width of the well,  $d_b$  is the barrier width,  $n_t$  is the total charge carrier concentration,  $\mu$  is the carrier mobility,  $E_F$  is the Fermi energy

Sample	$d_w$ , nm	$d_b$ , nm	$n_t$ , $10^{15} \text{ m}^{-2}$	$\mu$ , $\text{m}^2/(\text{V}\cdot\text{s})$	$E_F$ , meV	$k_F l$
DQW	5	10	2.27	1.13	9.4	17
SQW	10	0	2.10	1.21	8.6	12

The longitudinal  $\rho_{xx}(B, T)$  and Hall  $\rho_{xy}(B, T)$  components of the resistivity tensor are measured in a magnetic field  $B$  up to 2.5 T perpendicular to the 2D plane of the sample at fixed temperatures  $T = 1.8\text{--}20$  K in  $n\text{-In}_{0.2}\text{Ga}_{0.8}\text{As}/\text{GaAs}$  nanostructures with SQW and DQW quantum wells. Experiments were carried out at the Collaborative Access Center ‘‘Testing Center of Nanotechnology and Advanced Materials’’ of the M. N. Miheev Institute of Metal Physics of the Ural Branch of the Russian Academy of Sciences.

The experimental dependences  $\rho_{xx}(B, T)$  for a sample with a SQW are shown in Fig. 1. A ‘‘dielectric’’ behavior of the resistance with temperature changing occurs near weak fields  $B < 0.7$  T:  $\rho_{xx}(B, T)$  increases with decreasing  $T$  ( $\square$  in the inset to Fig. 1). The opposite behavior is observed beginning with a some value of  $B_c$ , i.e.,  $\rho_{xx}(B, T)$  increases with increasing temperature ( $\circ$  in the inset to Fig. 1). The change of the temperature behavior takes place at  $B \cong B_c$  near magnetic fields at  $\rho_{xx}(B, T) = \rho_{xy}(B, T)$ . We don’t see the single  $T_{ind}$ -point (like in the Fig. 3), it slightly diffuses into higher fields with increasing  $T$ . Shubnikov–de-Haas oscillations (with a filling factor  $\nu=8$ ) occur in the samples at  $B \approx 0.9$  T ( $B > B_c$ ). The negative magnetoresistance in magnetic fields  $B \lesssim B_c$  is associated with quantum interference corrections to the conductivity from weak localization.

The same features can be observed for the sample with DQW (Fig. 2). The only exception is the fact that the diffuse  $T_{ind}$ -point places in the region of Shubnikov–de-Haas oscillations.

Quantum effects are insignificant at high temperatures and low magnetic fields, so the conductivity can be calculated from the kinetic equation (Drude’s expression):

$$\begin{aligned} \sigma_{xx} &= \frac{\sigma_D}{1 + (\omega_c \tau)^2}, \\ \sigma_{xy} &= \omega_c \tau \sigma_{xx}. \end{aligned} \quad (1)$$

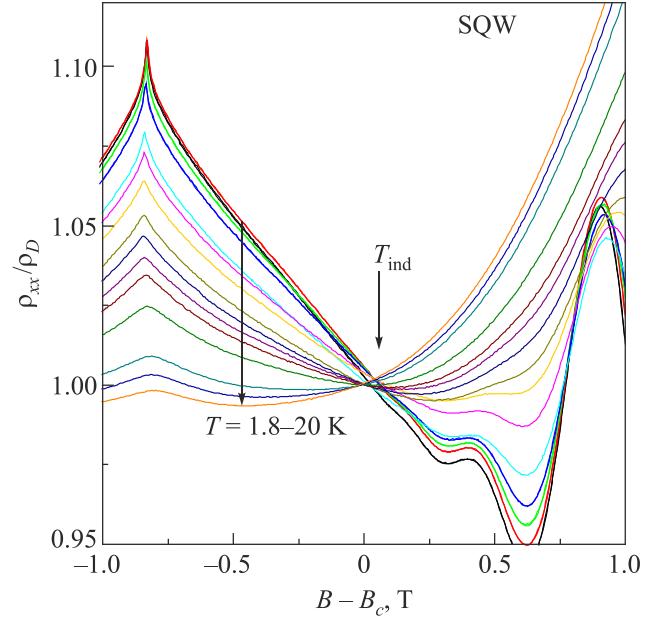


Fig. 3. (Color online) Dependencies  $\rho_{xx}/\rho_D$  on  $(B - B_c)$  at  $T = (1.8 - 20)$  K for SQW.

The conductivity in the absence of a magnetic field in weakly disordered 2D systems ( $k_F l \gg 1$ ) at low temperatures is determined by the Drude conductivity  $\sigma_D = e^2 k_F l / h$  and contributions from quantum interference corrections of two types  $\Delta\sigma = \Delta\sigma^{WL} + \Delta\sigma^{ee}$  (weak localization and electron-electron interaction). In the diffusion regime  $k_B T \tau / h \ll 1$  and in magnetic fields  $B > B_{tr} = h(4eD\tau)^{-1}$  ( $D$  is the diffusion coefficient), where the effects of weak localization are suppressed, the longitudinal magnetoresistance is given by the expression [21, 19]

$$\rho_{xx}(B, T) = \frac{1}{\sigma_D(T)} + \left\{ 1 - [\mu(T)B]^2 \right\} \frac{|\Delta\sigma_{ee}(T)|}{\sigma_D(T)^2}. \quad (2)$$

It is clear that  $\rho_{xx}$  depends on  $B$  in a quadratic manner and for  $\mu B = 1$  becomes independent on  $T$  (the so-called parabolic negative magnetoresistance model).

The experimental dependences  $\rho_{xx}(B)$  for the samples under study clearly demonstrate a diffusion of  $T_{ind}$ -point in temperature. It was shown in [22–24] that this diffusion is associated with the temperature dependence of the electron mobility  $\mu(T)$  which is determined by the temperature dependences of corrections to conductivity from the interference induced effects of weak localization and electron-electron interaction in  $k_B T \tau / h \ll 1$  temperature range ( $k_B$  — Boltzmann’s constant,  $h$  — Planck’s constant),  $\mu(T) \propto \ln(T)$  [20, 22], and from exchange contribution of electron-electron interaction (the interference contribution to the conductivity from scattering by Friedel oscillations) in  $k_B T \tau / h \gg 1$  temperature range,  $\mu(T) \propto T$  [24]. The growth of  $\mu(T)$  is essential:  $\Delta\mu/\mu(10 \text{ K}) \approx 40\%$  for DQW and  $\Delta\mu/\mu(10 \text{ K}) \approx (20\text{--}25)\%$  for SQW [24]. So, the interference-induced effects are significant in samples under study.

The critical behavior of the magnetoresistance in the  $\omega_c \tau \cong 1$  region was investigated in [15] where a rather rough method for accounting of the temperature dependence  $\mu(T)$  was used: the experimental values of  $\rho_{xx}(B, T)$  and  $\rho_{xy}(B, T)$  were inverted into the magnetoconductivity tensor [Eq. (1)], and then a series of curves  $\rho_{xx}^*(B, T)$  at different temperatures was calculated using Hall resistivity taken only at  $T = 1.8$  K,  $\rho_{xy}(B, T = 1.8$  K), at the reverse transformation. The genuine scaling properties were found with the critical exponent values depending on the density and mobility of the charge carriers: the lower the density the greater the deviations from the theoretically predicted values [15]. This fact points to the importance of the screening of charged impurity defects by conduction electrons and thus to electron-electron interactions.

Here we use another method of accounting of the temperature dependence  $\mu(T)$ . The data from Figs. 1 and 2 are set out in coordinates  $[(B - B_c); \rho_{xx} / \rho_D]$  (Figs. 3 and 4),  $B_c = 1/\mu$ ,  $\rho_D = 2/\sigma(B = B_c)$ , where at  $B_c$   $\sigma_{xx}(B_c) = \sigma_{xy}(B_c)$ . This allows us to take into account the dependence  $\mu(T)$  accurately.  $T_{\text{ind}}$ -point is perfectly visible (Figs. 3 and 4), which is in full accordance with Eq. (2). The results obtained allow us to conclude that the nature of the temperature-independent point is determined by the joint action of the classical cyclotron motion and quantum interference effects of weak localization and electron-electron interaction.

The  $\mu(T)$  accounting method used indicates that in our case the  $T_{\text{ind}}$ -point position coincides with the magnetic field value which is the boundary between classical and quantizing magnetic fields. For the DQW sample the  $T_{\text{ind}}$ -point position is also before the region of Shubnikov–de-Haas oscillations (Fig. 4).

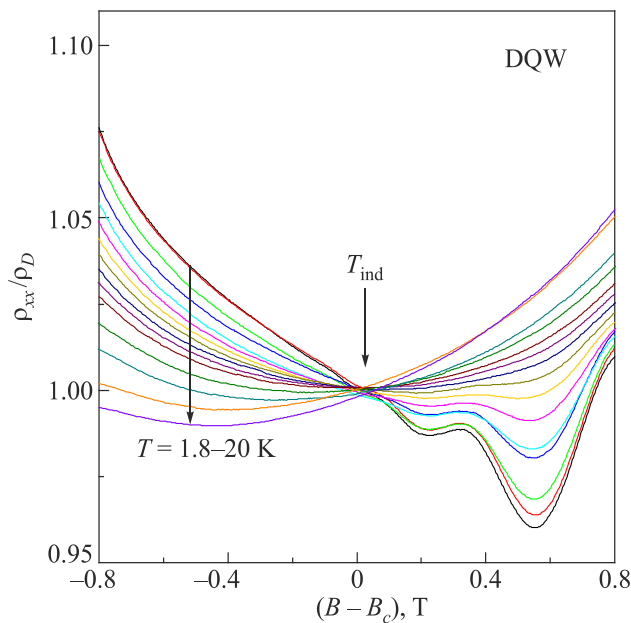


Fig. 4. (Color online) Dependencies  $\rho_{xx}/\rho_D$  on  $(B - B_c)$  at  $T = (1.8\text{--}20)$  K for DQW.

Tunable insulator-quantum Hall transition was demonstrated in [8] by using gate voltage as a tool for shifting the  $\rho_{xx}(B) = \rho_{xy}(B)$  position with respect to  $T_{\text{ind}}$ -point by varying the effective amount of disorder and the carrier density in GaAs/AlGaAs structures with long-range scattering potential which was used for suppressing electron interaction. The conclusion [8] is that at least for the system with weak electron-electron interaction the onset of strong localization occurs at a relatively higher field that does not correspond to  $B_c = 1/\mu$ , a boundary between classical and quantizing magnetic fields as it is in our experiments.

According to conclusions in [5] a quantum phase transition from the dielectric phase to the QHE phase is possible when only a plateau with  $n=1$  ( $\nu=1$ ) in the QHE mode is observed. In this case, the classical conductivity [Eq. (1)] can be  $\sim e^2/2h$  during the QHE-dielectric phase transition in low magnetic fields and the scale of crossover  $\xi$  can be microscopic. Then a scaling behavior should be observed at the  $T_{\text{ind}}$ -point [18].

A phase diagram is drawn to show conditions for transition occurrence from the dielectric phase to the QHE phase in our system (Fig. 5). This diagram is an analogue of the global QHE phase diagram [3]. Depending on degree of disorder in the system the transition from the dielectric phase to the QHE phase can occur both through the intermediate phases of the quantum Hall liquid, corresponding to the filling factors  $\nu > 1$ , and directly into the phase with  $\nu = 1$  [18]. It is clear that there are two QHE phases with

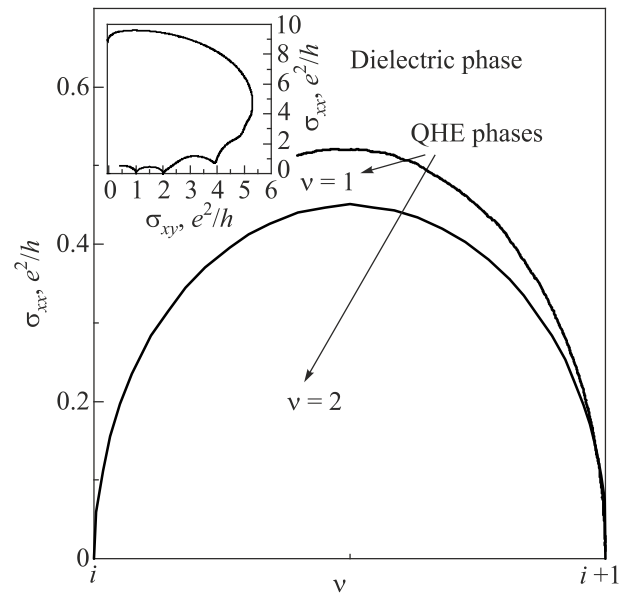


Fig. 5. According to [3] the part of the QHE phase diagram of the  $n\text{-In}_{0.2}\text{Ga}_{0.8}\text{As}/\text{GaAs}$  structure with a SQW at  $T = 0.05$  K, obtained in magnetic fields up to 16 T. The break of the line separating the dielectric phase and the QHE phase with  $\nu = 1$  corresponds to the achievement of limiting values of the magnetic fields in the experimental installation. Inset:  $\sigma_{xx}(\sigma_{xy})$  dependence at  $T = 0.05$  K.



$\nu = 2$  and  $\nu = 1$  in our system, so, according to [5], we assume that there is the crossover at the  $T_{\text{ind}}$ -point, which confirms our conclusions regarding its origin.

We would like to emphasize that the found peak values of  $\sigma_{xx} = 0.45e^2/h$  for  $\nu = 2$  и  $\sigma_{xx} = 0.52e^2/h$  for  $\nu = 1$  (Fig. 5) well correspond to the predictions of the theory (see, for example, review [25], which up to now have been observed experimentally only in several cases (see references in [26]). That characterizes the systems studied as an ideal model object.

### Conclusions

It has been experimentally shown that in the structures with strong interference-induced effects and a short-range disorder potential the origin of the temperature-independent point on the set of  $\rho_{xx}(B, T)$  curves located at  $\omega_c \tau \cong 1$  is associated with the joint action of the classical cyclotron motion and quantum interference effects of weak localization and electron-electron interaction. In structures studied the transition from the dielectric phase to the phase of the quantum Hall effect is a crossover from weak localization (quantum interference effects in a low magnetic field) to strong localization in quantizing magnetic fields in the QHE regime.

The research was carried out within the state assignment of Ministry of Science and Higher Education of the Russian Federation (theme “Electron” No. AAAA-A18-118020190098-5), supported in part by the Russian Foundation for Basic Research, grant No. 18-02-00192. Experiments were carried out at the Collaborative Access Center “Testing Center of Nanotechnology and Advanced Materials” of the M. N. Miheev Institute of Metal Physics of the Ural Branch of the Russian Academy of Sciences.

1. D. E. Khmel'nitskii, *Phys. Lett. A* **106**, 182 (1984).
2. R. B. Laughlin, *Phys. Rev. Lett.* **52**, 2304 (1984).
3. S. A. Kivelson, D.-H. Lee, and Sh.-Ch. Zhang, *Phys. Rev. B* **46**, 2223 (1992).
4. V. T. Dolgoplov, *Phys. Usp.* **57**, 105 (2014).
5. Bodo Huckestein, *Phys. Rev. Lett.* **84**, 3141 (2000).
6. E. Abrahams, P. W. Anderson, D. C. Licciardello, and T. V. Ramakrishnan, *Phys. Rev. Lett.* **42**, 673 (1979).
7. W. Pan, K. W. Baldwin, K. W. West, L. N. Pfeiffer, and D. C. Tsui, *Phys. Rev. B* **94**, 161303(R) (2016).
8. Shun-Tsung Lo, Yi-Ting Wang, Sheng-Di Lin, Gottfried Strasser, Jonathan P. Bird, Yang-Fang Chen, and Chi-Te Liang, *Nanoscale Research Lett.* **8**, 307 (2013).
9. Shun-Tsung Lo, Yi-Ting Wang, G. Bohra, E. Comfort, T.-Y. Lin, M.-G. Kang, G. Strasser, J. P. Bird, C. F. Huang, Li-Hung Lin, J. C. Chen, and C.-T. Liang, *J. Phys.: Condens. Matter* **24**, 405601 (2012).
10. C. H. Lee, Y. H. Chang, Y. W. Suen, and H. H. Lin, *Phys. Rev. B* **56**, 15238 (1997).
11. D. R. Hang, C. F. Huang, Y. W. Zhang, H. D. Yeh, J. C. Hsiao, and H. L. Pang, *Solid State Commun.* **141**, 17 (2007).
12. Gil-Ho Kim, C.-T. Liang, C. F. Huang, J. T. Nicholls, D. A. Ritchie, P. S. Kim, C. H. Oh, J. R. Juang, and Y. H. Chang, *Phys. Rev. B* **69**, 073311 (2004).
13. K. H. Gao, G. Yu, Y. M. Zhou, L. M. Wei, T. Lin, L. Y. Shang, L. Sun, R. Yang, W. Z. Zhou, N. Dai, J. H. Chu, D. G. Austing, Y. Gu, and Y. G. Zhang, *J. Appl. Phys.* **108**, 063701 (2010).
14. Shun-Tsung Lo, Chang-Shun Hsu, Y. M. Lin, S.-D. Lin, C. P. Lee, Sheng-Han Ho, Chiashain Chuang, Yi-Ting Wang, and C.-T. Liang, *Appl. Phys. Lett.* **105**, 012106 (2014).
15. A. P. Savelyev, S. V. Gudina, Yu. G. Arapov, V. N. Neverov, S. M. Podgornykh, and M. V. Yakunin, *Fiz. Nizk. Temp.* **43**, 612 (2017) [*Low Temp. Phys.* **43**, 491 (2017)].
16. Fan-Hung Liu, Chang-Shun Hsu, Chiashain Chuang, Tak-Pong Woo, Lung-I Huang, Shun-Tsung Lo, Yasuhiro Fukuyama, Yanfei Yang, Randolph E. Elmquist, and Chi-Te Liang, *Nanoscale Research Lett.* **8**, 360 (2013).
17. E. Pallecchi, M. Ridene, D. Kazazis, F. Lafont, F. Schopfer, W. Poirier, M. O. Goerbig, D. Mailly, and A. Ouerghi, *Sci. Rep.* **3**, 1791 (2013).
18. S.-H. Song, D. Shahar, D. C. Tsui, Y. H. Xie, Don Monroe, *Phys. Rev. Lett.* **78**, 2200 (1997).
19. Yu. G. Arapov, G. I. Harus, O. A. Kuznetsov, V. N. Neverov, and N. G. Shelushinina, *Semiconductors* **33**, 1073 (1999).
20. Yu. G. Arapov, S. V. Gudina, V. N. Neverov, S. M. Podgornykh, A. P. Savelyev, and M. V. Yakunin, *Fiz. Nizk. Temp.* **41**, 289 (2015) [*Low Temp. Phys.* **41**, 221 (2015)].
21. M. A. Paalanen, D. C. Tsui, and J. C. M. Hwang, *Phys. Rev. Lett.* **51**, 2226 (1983).
22. Yu. G. Arapov, S. V. Gudina, I. V. Karskanov, V. N. Neverov, G. I. Harus, and N. G. Shelushinina, *Fiz. Nizk. Temp.* **33**, 222 (2007) [*Low Temp. Phys.* **33**, 160 (2007)].
23. Yu. G. Arapov, I. V. Karskanov, G. I. Harus, V. N. Neverov, N. G. Shelushinina, and M. V. Yakunin, *Fiz. Nizk. Temp.* **35**, 44 (2009) [*Low Temp. Phys.* **35**, 32 (2009)].
24. S. V. Gudina, Yu. G. Arapov, V. N. Neverov, A. P. Savelyev, S. M. Podgornykh, N. G. Shelushinina, and M. V. Yakunin, *Physica E: Low Dimens. Syst. Nanostruct.* **113**, 14 (2019).
25. A. M. M. Pruisken, *Int. J. Modern Phys. B* **24**, 1895 (2010).
26. Yu. G. Arapov, S. V. Gudina, A. S. Klepikova, V. N. Neverov, G. I. Harus, N. G. Shelushinina, and M. V. Yakunin, *Semiconductors* **51**, 272 (2017).

Локалізація та квантові інтерференційні ефекти  
в слабких магнітних полях  
у структурах InGaAs/GaAs

A. P. Savelyev, Yu. G. Arapov, S. V. Gudina,  
V. N. Neverov, S. M. Podgornykh,  
N. G. Shelushinina, M. V. Yakunin

Експериментально досліджено поздовжній  $\rho_{xx}(B, T)$  та холлівський  $\rho_{xy}(B, T)$  опори в наноструктурах  $n$ -InGaAs/GaAs з одиничними та подвійними квантовими ямами в діапазоні магнітних полів  $B = 0$ – $2.5$  Тл та температур  $T = 1.8$ – $20$  К. Показано, що походження температурно-незалежної точки,

що знаходиться поблизу  $\omega_c\tau \cong 1$  на кривих  $\rho_{xx}(B, T)$ , пов'язане зі спільною дією класичного циклотронного руху та квантових інтерференційних ефектів слабкої локалізації й електрон-електронної взаємодії. Отримані результати свідчать, що перехід з діелектричної фази у фазу квантового ефекту Холла є кросовером від слабкої локалізації (квантові інтерференційні ефекти в слабкому магнітному полі) до сильної локалізації при квантуванні магнітних полів у режимі квантового ефекту Холла.

Ключові слова: квантовий ефект Холла, кросовер, квантова інтерференція.